Supplementary Materials for

The Microanatomic Segregation of Selection by Apoptosis in the Germinal Center

Christian T. Mayer, Anna Gazumyan, Ervin E. Kara, Alexander D. Gitlin, Jovana Golijanin, Charlotte Viant, Joy Pai, Thiago Y. Oliveira, Qiao Wang, Amelia Escolano, Max Medina-Ramirez, Rogier W. Sanders and Michel C. Nussenzweig

correspondence to: nussen@rockefeller.edu

This PDF file includes:

Other Supplementary Materials for this manuscript includes the following:

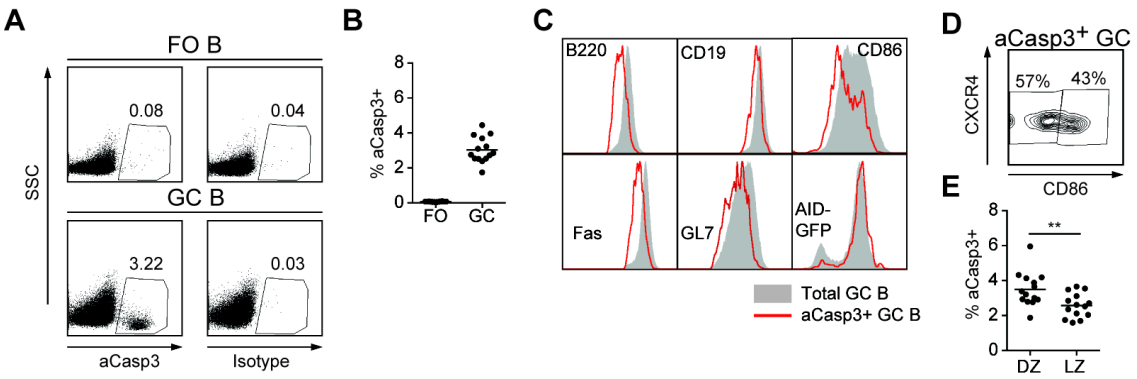

Fig. S1.

Cell death in GC B cells. Peyer's patches of C57BL/6 mice were analyzed by flow cytometry. (**A**) Representative flow cytometry plots show aCasp3 staining (left column) or isotype control staining (right column) and SSC among FO B cells (top) or GC B cells (bottom). (**B**) Percentages of aCasp3$^+$ FO B cells and aCasp3$^+$ GC B cells. (**C**) Histograms show expression levels of indicated markers on total GC B cells (grey solid histograms) and aCasp3$^+$ GC B cells (red lines). Peyer's patches from *AID*-GFP transgenic mice were used to assess AID expression. (**D**) Representative CD86 and CXCR4 staining of aCasp3$^+$ GC B cells. (**E**) Percentage of aCasp3$^+$ cells in the GC DZ (CD86^{lo}CXCR4^{hi}) or LZ (CD86^{hi}CXCR4^{lo}). (**A-E**). Data are from four independent experiments each involving 2-4 mice. Expression levels of B220, Fas and *AID*-GFP are from at least two independent experiments. ** p = 0.0079, unpaired two-tailed Student's *t*-test.

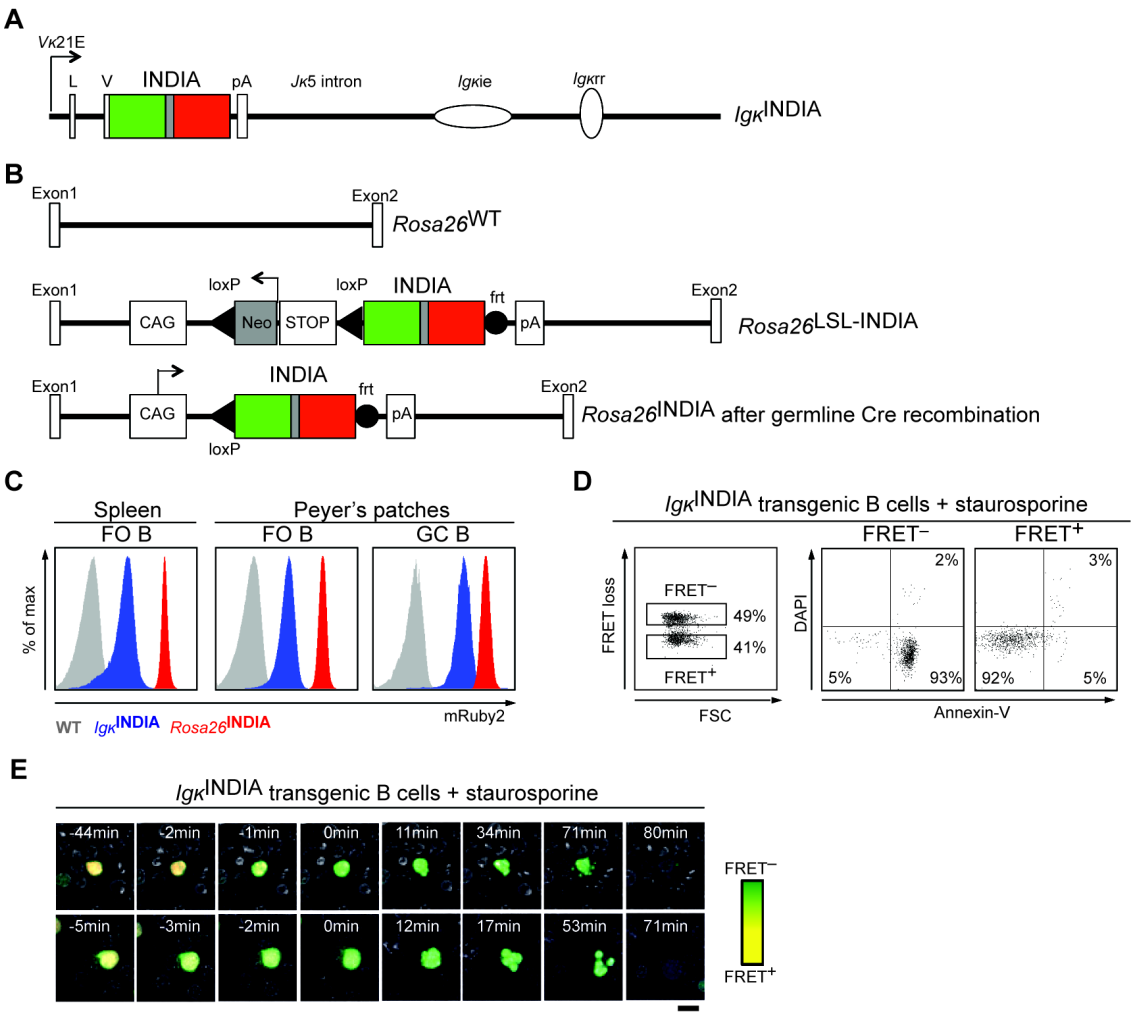

Fig. S2

Apoptosis reporter mice. (**A**) Schematic illustration of the 7.2kb *Igκ*^{INDIA} transgene. INDIA cDNA is embedded into mouse *Igκ* regulatory elements (*Vκ21E* promoter, non-coding leader (L) and V gene exons, polyadenylation signal (pA), intronic sequence with enhancer (ie), and 3' regulatory region (rr)). (**B**) Top: Schematic illustration of the wildtype *Rosa26* genomic region spanning non-coding exons 1 and 2 (*Rosa26*^{WT}). Middle: targeted *Rosa26* locus in knock-in mice retaining a loxP-flanked STOP cassette (*Rosa26*$^{LSL\text{-}INDIA}$; CAG: CMV enhancer, chicken β-actin promoter and rabbit β-globin splice acceptor; Neo: neomycin; STOP: STOP cassette preventing INDIA expression; pA: polyadenylation signal). Bottom: targeted *Rosa26* locus in knock-in mice following germline Cre-mediated recombination (*Rosa26*^{INDIA}). (**C**) Splenocytes and Peyer's patches of WT mice, *Igκ*^{INDIA} transgenic mice and *Rosa26*^{INDIA} knock-in mice were analyzed by flow cytometry. INDIA expression was assessed in FO B cells and GC B cells by direct 561-nm excitation of mRuby2. Results are representative for 2-3 independent experiments. (**D**) Splenic B cells were purified from *Igκ*^{INDIA} transgenic mice, activated in vitro with LPS and IL-4 for 4 d and incubated with staurosporine for 3 h. Cells were then analyzed by flow cytometry. Left flow cytometry plot shows FSC and FRET loss of mRuby2^{+} cells. FRET^{+} and FRET$^{–}$ cells were gated and assessed for

Annexin-V binding and DAPI permeability. One out of two independent experiments is shown. (**E**) Activated *Igκ*^{INDIA} B cells were imaged at 37ºC after addition of 1 μM staurosporine. Representative images of two INDIA^{+} B cells are shown over time (yellow, FRET^{+}; green, FRET$^{–}$; scale bar: 10 μm). FRET loss was synchronized to 0 min. Data are from two independent experiments each containing ten imaging fields.

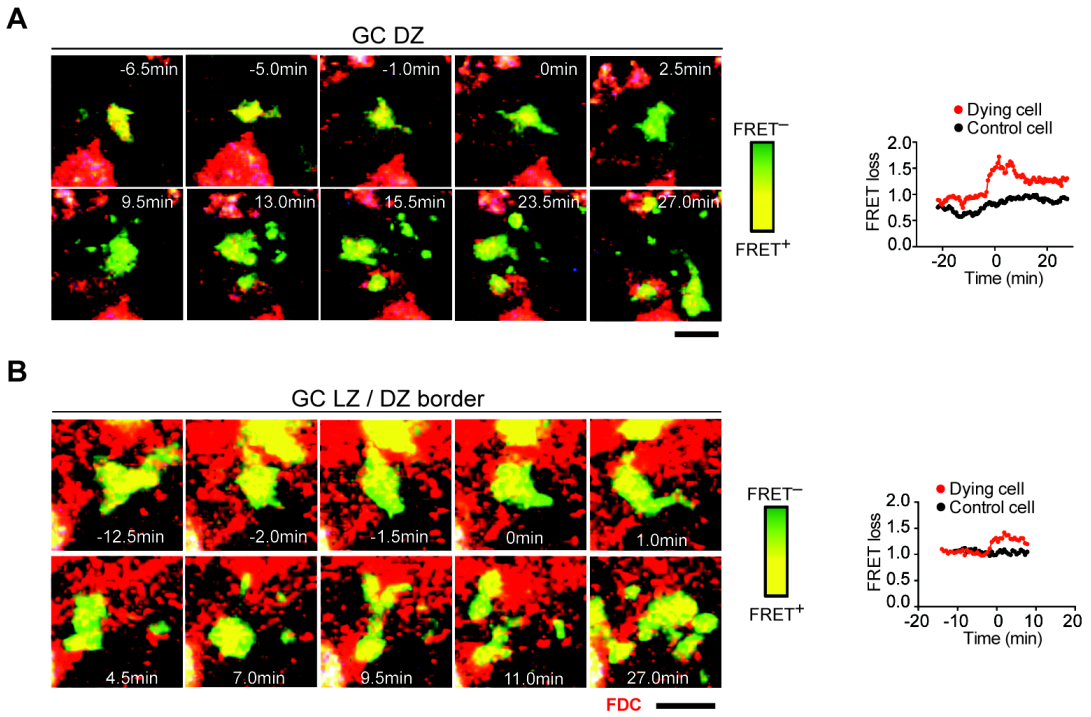

Fig. S3

Apoptotic GC B cells in lymph nodes. NP-specific GCs were elicited by immunizing OVA-primed mice that received B1-8^{hi} B cells (5% *Rosa26*^{INDIA} / 95% *Rosa26*^{WT}). Popliteal lymph nodes were imaged by two-photon laser scanning microscopy. FDC networks of the GC LZ were visualized with fluorescent immune complexes containing B-PE (red). (**A and B**, left) Collapsed Z-stacks of 30-µm depth (5-µm steps) depict GC B cells dying over time (yellow: FRET^{+}; green: FRET^{-}; scale bar: 10 µm). (**A**) DZ (an autofluorescent tingible body macrophage is noted at the bottom). (**B**) Border area of LZ and DZ. (**A and B**, right) FRET loss ratios of the same dying GC B cells were tracked over time (red lines). FRET loss is synchronized to 0 min. FRET loss ratios of a live GC B-cell were tracked within the same imaging volumes, respectively (black lines). Data are from three experiments and six independently imaged mice.

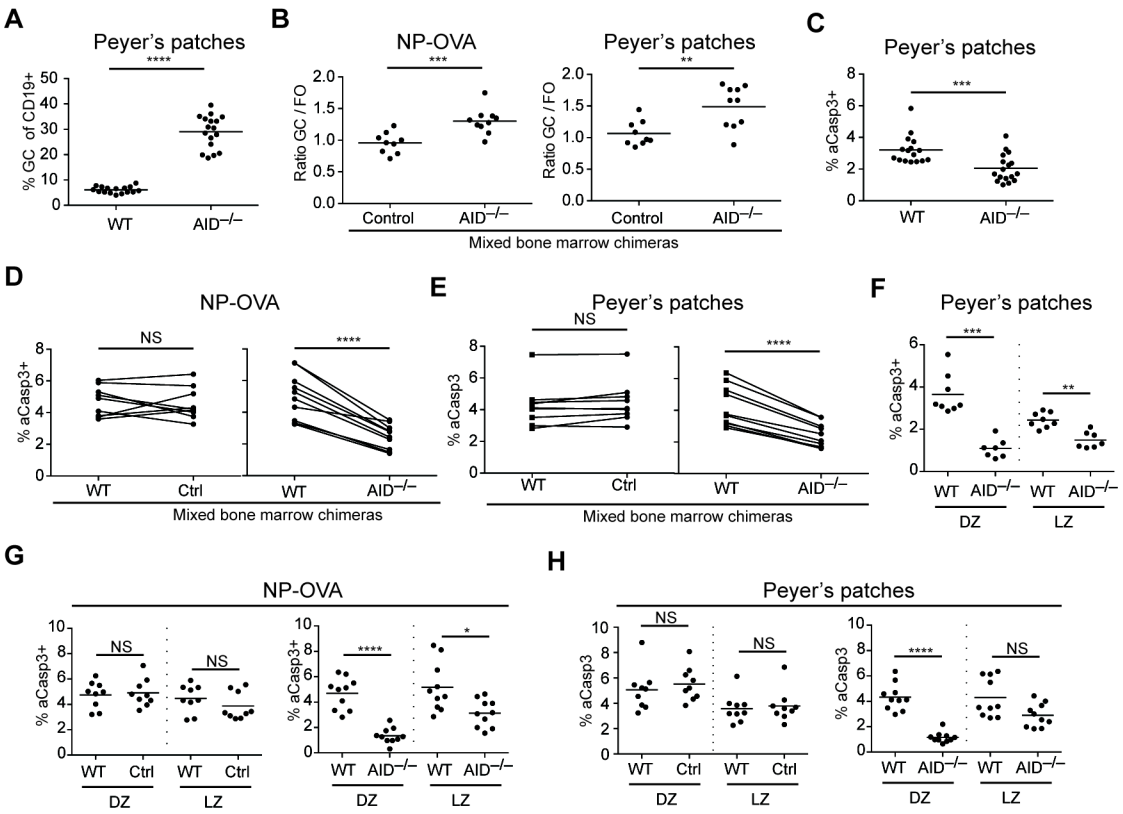

Fig. S4

AID contributes to GC B-cell apoptosis in the DZ. (**A**) Peyer's patches of C57BL/6 (WT) or AID$^{-/-}$ mice were analyzed by flow cytometry. Percentage of GC B cells among CD19^{+} B cells. Each dot represents a mouse. **** $p < 0.0001$; two-tailed Mann-Whitney U test. (**B**) Bone marrow chimeras. Lethally irradiated C57BL/6 mice received a mixture of CD45.2^{+} WT and CD45.1^{+} AID$^{-/-}$ bone marrow (50%/50%). Control chimeras received a mixture of CD45.2^{+} WT and CD45.1^{+} WT bone marrow cells (50%/50%). Eight weeks after reconstitution, mice were immunized with NP-OVA precipitated in alum. Fourteen days later, draining lymph nodes, and Peyer's patches were analyzed by flow cytometry. The ratios of CD45.1^{+} GC B-cell and CD45.1^{+} FO B-cell frequencies were calculated for control chimeras (Control) and experimental chimeras (AID$^{-/-}$). ** $p = 0.004$, *** $p = 0.0009$; unpaired two-tailed Student's *t*-test. (**C**) Quantitation of aCasp3^{+} cells among Peyer's patch GC B cells of WT and AID$^{-/-}$ mice. *** $p = 0.0003$; two-tailed Mann-Whitney U test. (**D, E**) Quantitation of aCasp3^{+} cells among Peyer's patch GC B cells or lymph node GC B cells in NP-OVA-immunized control chimeras (CD45.2^{+} WT and CD45.1^{+} WT Ctrl) or experimental chimeras (CD45.2^{+} WT and CD45.1^{+} AID$^{-/-}$). **** $p < 0.0001$; NS, not statistically significant, paired two-tailed Student's *t*-test. (**F**) Quantitation of aCasp3^{+} DZ and LZ GC B cells from Peyer's patches of WT and AID$^{-/-}$ mice. *** $p = 0.0003$, ** $p = 0.0012$; two-tailed Mann-Whitney U test. (**G**) Quantitation of aCasp3^{+} DZ and LZ GC B cells in draining lymph nodes of NP-OVA-immunized control chimeras (CD45.2^{+} WT and CD45.1^{+} WT Ctrl) and experimental chimeras (CD45.2^{+} WT and CD45.1^{+} AID$^{-/-}$). **** $p < 0.0001$; * $p = 0.0115$; NS, not statistically significant, two-tailed Mann-Whitney U test. (**H**)

Quantitation of aCasp3^{+} DZ and LZ GC B cells in Peyer's patches of control chimeras (CD45.2^{+} WT and CD45.1^{+} WT Ctrl) and experimental chimeras (CD45.2^{+} WT and CD45.1^{+} AID$^{-/-}$). **** $p < 0.0001$; NS, not statistically significant, two-tailed Mann-Whitney U test. (**A, C**) Data are pooled from four experiments each involving 3-5 mice per genotype. (**B, D, E-H**) Data are from two independent experiments each involving four mice per genotype.

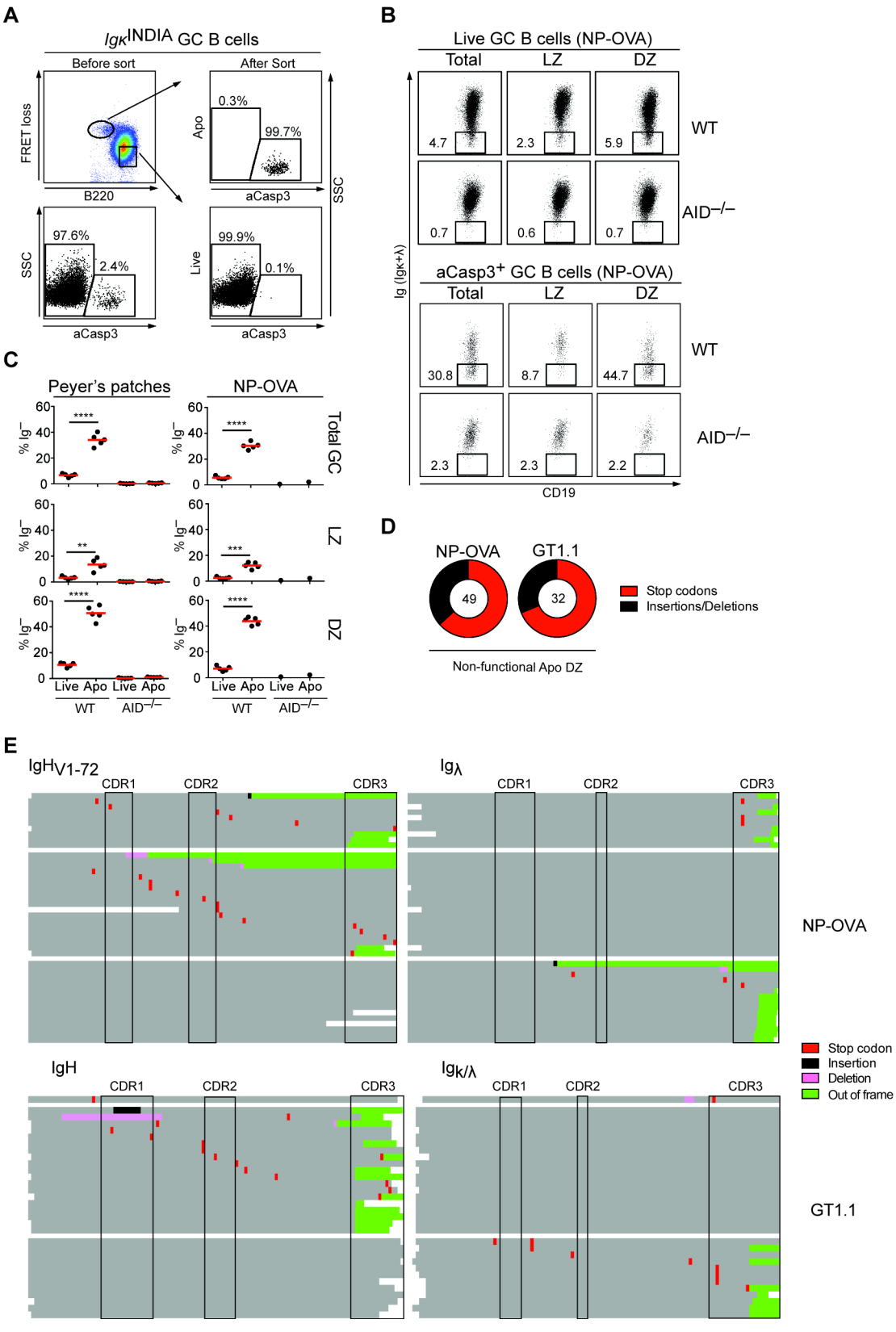
A
IgκINDIA GC B cells
Before sort
After Sort
FRET loss
B220
Apo
aCasp3
SSC
0.3%
99.7%
97.6%
2.4%
Live
99.9%
0.1%
B
Live GC B cells (NP-OVA)
Total
LZ
DZ
WT
AID−/−
4.7
2.3
5.9
0.7
0.6
0.7
aCasp3+ GC B cells (NP-OVA)
Ig (Igκ+λ)
CD19
30.8
8.7
44.7
2.3
2.3
2.2
C
Peyer's patches
NP-OVA
% Ig−
Total GC
LZ
DZ
Live Apo Live Apo
WT
AID−/−
D
NP-OVA
GT1.1
49
32
Stop codons
Insertions/Deletions
Non-functional Apo DZ
E
IgHV1-72
Igλ
CDR1
CDR2
CDR3
NP-OVA
IgH
Igk/λ
GT1.1
Stop codon
Insertion
Deletion
Out of frame

Fig. S5

Selection against BCR loss in the GC DZ. (**A**) *Igκ*^{INDIA} transgenic mice were immunized with NP-OVA precipitated in alum. After 14 d, spleens and lymph nodes were harvested and GC B cells were enriched and stained with fluorophore-conjugated antibodies. B220^{+}DUMP^{-}CD38^{-}Fas^{+}mRuby2^{+} live (B220^{+}FRET^{+}) or apoptotic (B220^{lo}FRET^{-}) GC B-cell fractions were sorted by FACS followed by flow cytometry. Upper left plot shows B220 expression and FRET loss of GC B cells before sorting. aCasp3 staining and SSC are shown prior to (left bottom) and after FACS sorting (right panel). One out of two independent experiment is shown. (**B, C**) Draining lymph nodes from NP-OVA-immunized WT and AID$^{-/-}$ mice (d 14), or Peyer's patches were analyzed by flow cytometry. (**B**) Representative dot plots show CD19 and Ig (surface + intracellular Igκ/λ) expression of indicated GC B-cell population after NP-OVA immunization. Top panel: aCasp3^{-} GC B cells; bottom panel: aCasp3^{+} GC B cells. Total GC (left column), CXCR4^{lo}CD86^{hi} LZ (middle column) and CXCR4^{hi}CD86^{lo} DZ (right column) are shown for WT and AID$^{-/-}$ mice. Numbers indicate percentages of Ig^{-} GC B cells. (**C**) Percentages of Ig^{-} GC B-cell populations are summarized for Peyer's patches (left column) and after NP-OVA immunization (right column). Total GC (top row), LZ (middle row) and DZ (bottom row) are shown. One out of 2-3 independent experiments each involving five (NP-OVA), 4-5 (WT Peyer's patches) and 1-5 (AID$^{-/-}$ Peyer's patches) mice. (**D, E**) *Igκ*^{INDIA} transgenic mice were immunized with NP-OVA or GT1.1. Apoptotic DZ (B220^{lo}FRET^{-}CXCR4^{hi}CD86^{lo}) GC B cells were single-cell-sorted 14 d after immunization. After cDNA preparation, *IgH, Igλ* and *Igκ* chains were amplified and sequenced. (**D**) Fractions of stop codons (red) and insertions/deletions (black) in non-functional paired *Ig* sequences. *Igλ/Igκ* sequences were only assessed in case of a functional or ambiguous *IgH*. In case of multiple lesions within one *Ig* gene, the first 5' event altering BCR expression was counted. (**E**) Positions and types of all BCR lesions in paired non-functional *IgH* (left) and *Igλ/Igκ (right)* sequences after NP-OVA (top) and GT1.1 (bottom) immunization. Stop codon (red), insertion (black), deletion (pink), out-of-frame (green). (**D, E**) Data are accumulated from ten (NP-OVA) and four (GT1.1) independent experiments. **** $p < 0.0001$, *** $p = 0.0004$, ** $p = 0.0038$; paired two-tailed Student's *t*-test.

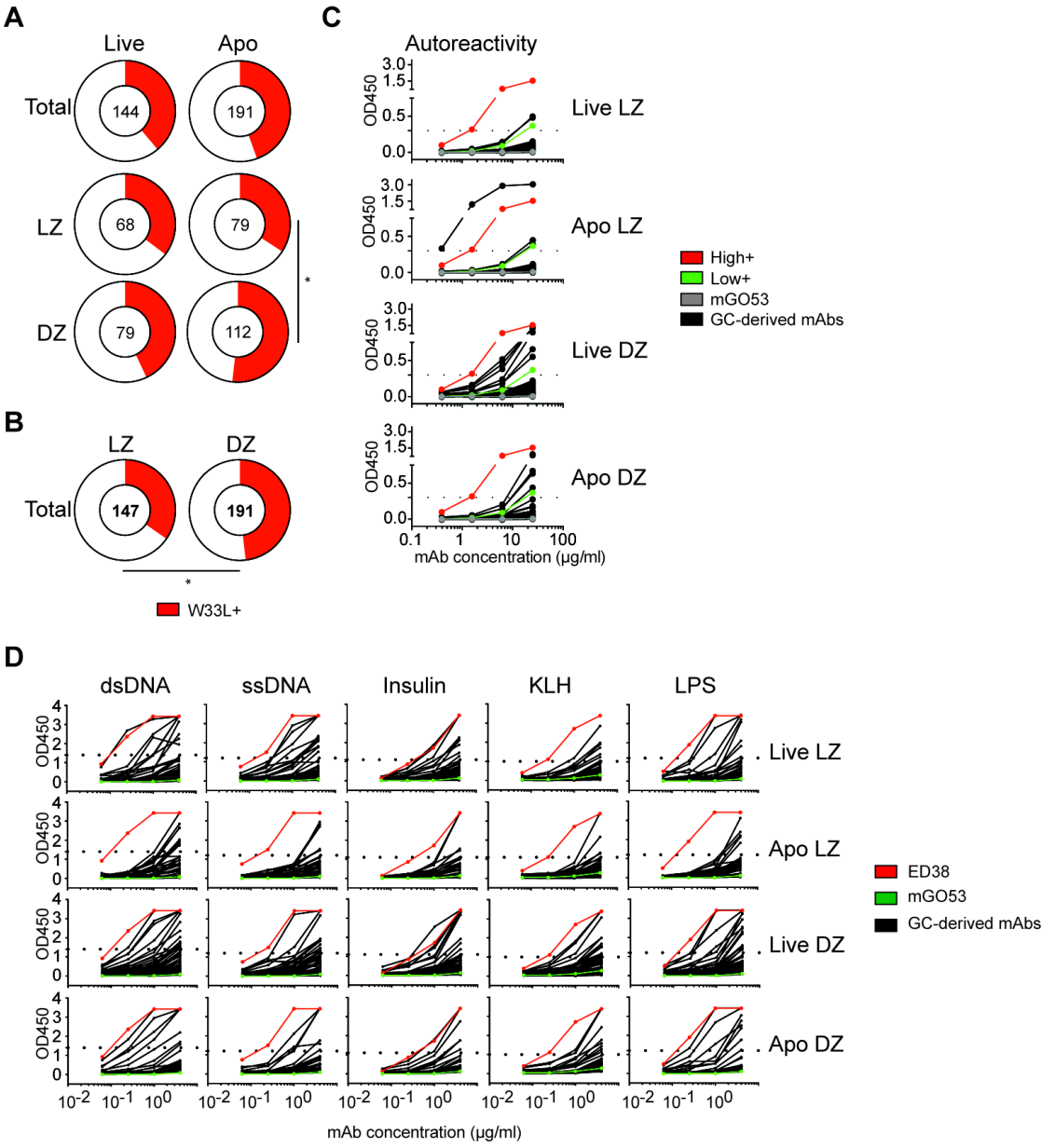

Fig. S6

GC-derived $IgH_{V1\text{-}72}$ Ig_{λ} antibodies. (**A**) In-frame *$IgH_{V1\text{-}72}$* sequences of indicated GC B-cell populations were analyzed for the presence of the affinity-enhancing W33L mutation (red). (**B**) Same as in (**A**) but for all LZ and DZ cells irrespective of cell death. * p = 0.0183 (Apo LZ vs Apo DZ), * p = 0.0146 (total LZ vs total DZ), Fisher's exact test. Sequences are derived from ten independent experiments. (**C**) Binding of GC-derived monoclonal antibodies to nuclear and cytoplasmic self-antigens by ELISA. High-positive (red), low-positive (green) and negative controls (mGO53, grey) are shown. Horizontal lines mark positive reactivity. Every autoreactive antibody was confirmed by two independent ELISA measurements. (**D**) Binding of GC-derived monoclonal antibodies to

dsDNA, ssDNA, insulin, KLH, and LPS by ELISA. The highly polyreactive antibody ED38 served as a positive control. mGO53 is included as a negative control. Horizontal lines indicate cutoffs for positive reactivity.

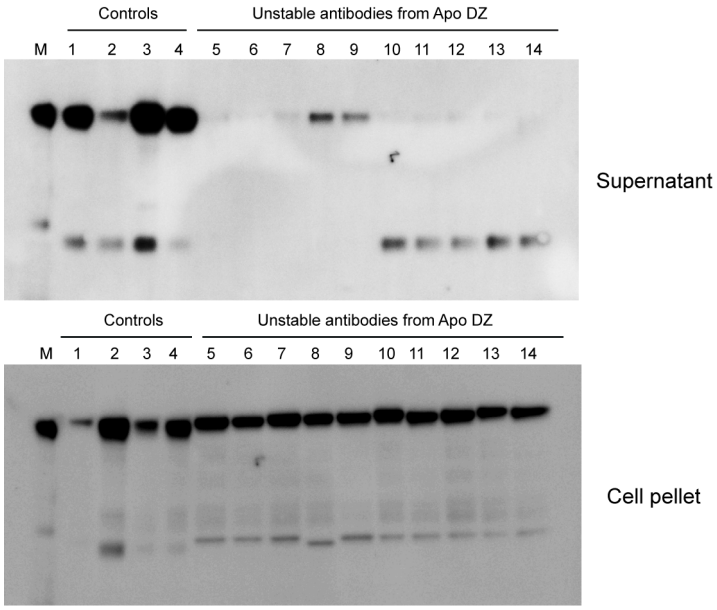

Fig. S7

Unstable antibodies in the apoptotic GC DZ. *Ig* genes were cloned from live and apoptotic GC DZ and LZ compartments after NP-OVA immunization. HEK293-6E cells were transfected to produce GC-derived $IgH_{V1\text{-}72}$ Ig_{λ} antibodies. Immunoblot was performed to detect Ig chains in the supernatant (top) or cell pellets (bottom) 7 d after transfection. Representative blots show control $IgH_{V1\text{-}72}$ Ig_{λ} antibodies cloned from live and apoptotic LZ and DZ GC compartments (lanes 1-4) and unstable antibodies cloned from the apoptotic DZ (lanes 5-14). In total, 23 unstable antibodies from the apoptotic DZ were assessed in two independent experiments (M, marker spiked with control antibody).

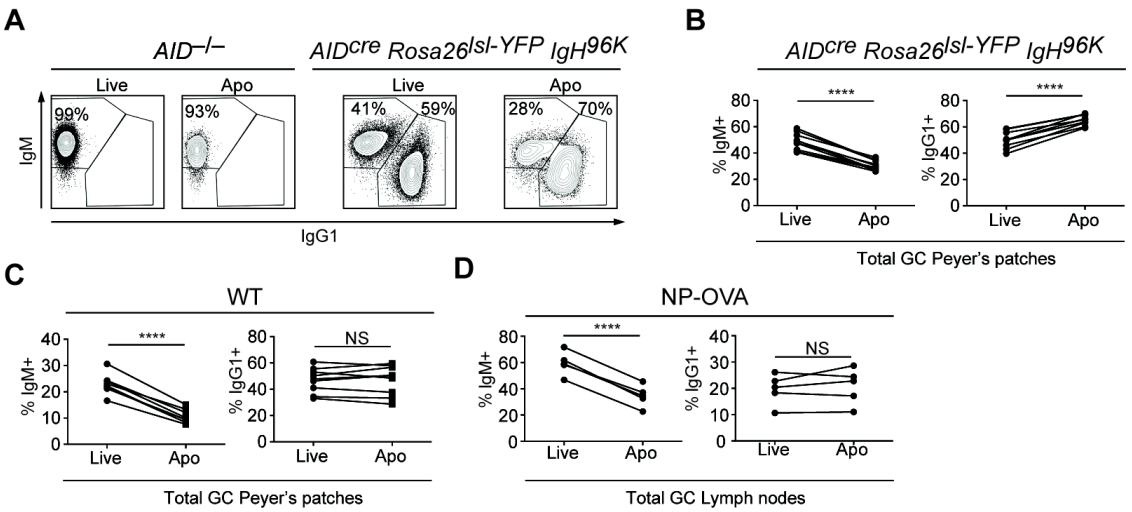

Fig. S8

IgG1 isotype promotes GC B-cell apoptosis independent of SHM. (**A, B**) Peyer's patches of *AID*$^{-/-}$ or *AID*$^{Cre/Cre}$*Rosa26*$^{lsl\text{-}YFP}$*IgH*$^{96K/96K}$ mice were analyzed by flow cytometry. (**A**) Representative contour plots show IgG1 and IgM expression in aCasp3^{-} (Live) and aCasp3^{+} (Apo) total GC B cells. (**B**) Fractions of IgM^{+} and IgG1^{+} live and apoptotic GC B cells in *AID*$^{Cre/Cre}$*Rosa26*$^{lsl\text{-}YFP}$*IgH*$^{96K/96K}$ mice. (**A, B**) Results are combined from two independent experiments each involving 4-5mice per genotype. **** $p < 0.0001$; paired Student's *t*-test. (**C**) Peyer's patches or (**D**) draining lymph nodes of C57BL/6 mice 14 d after NP-OVA immunization were analyzed by flow cytometry. Fractions of IgM^{+} and IgG1^{+} live and apoptotic total GC B cells are shown. **** $p < 0.0001$, paired Student's *t*-test. (**C, D**) Results combine or represent two independent experiments each involving 4-5 mice per genotype.

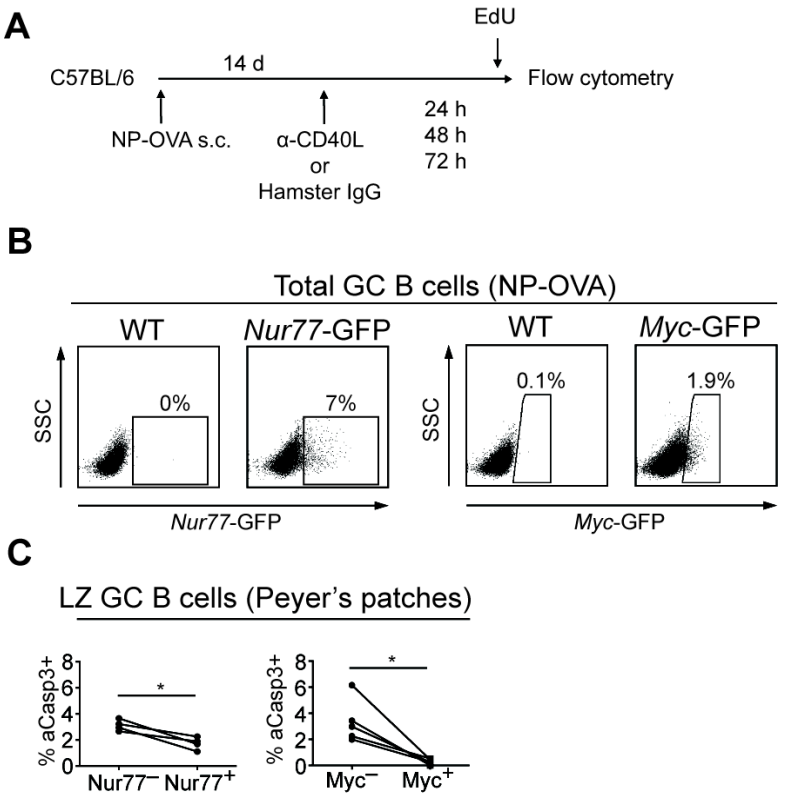

Fig. S9

Default apoptosis in the GC LZ. (**A**) Experimental schematic. C57BL/6 mice were immunized subcutaneously with NP-OVA precipitated in alum. After 14 d, draining lymph nodes were analyzed by flow cytometry. Mice were injected intravenously with hamster IgG or α-CD40L 24 h, 48 h or 72 h earlier, and were pulsed with 1 mg of EdU intravenously 1.0-2.5 h prior to analysis. (**B**) *Nur77*-GFP and *Myc*-GFP mice were immunized with NP-OVA subcutaneously. GC B cells were analyzed 14 d later in draining lymph nodes by flow cytometry and gated as $CD19^{+}CD38^{-}GL7^{+}Fas^{+}$. Representative dot plots show *Nur77*-GFP or *Myc*-GFP expression and SSC in total GC B cells. An immunized WT mouse is shown as control. (**C**) Peyer's patches of *Nur77*-GFP and *Myc*-GFP mice were assessed by flow cytometry. Frequencies of $aCasp3^{+}$ cells in LZ ($CXCR4^{lo}$ $CD86^{hi}$) GC B cells comparing *Nur77*-GFP^{-} and *Nur77*-GFP^{+} fractions (left graph), or *Myc*-GFP^{-} and *Myc*-GFP^{+} fractions (right graph). (**B, C**) Two independent experiments each involving six *Nur77*-GFP mice are shown. Three *Nur77*-GFP mice were pooled per data set. * p = 0.0197, paired Student's *t*-test. For *Myc*-GFP mice, four independent experiments each involving 3-6 mice are shown. Three *Myc*-GFP mice were pooled per data set. * p = 0.0143, paired Student's *t*-test.

Table S1.

Primers used to detect INDIA by PCR.

Primer number	Description	5'-Primer sequence-3'	Product size
263	mRuby2 fw	CCTGGCCACCTCATTCATGT	280 bp
264	mRuby2 rv	GGCAGGGTACATCATCTCGG	
265	mRuby2 fw	GATGTACCCTGCCGATGGAG	258 bp
266	mRuby2 rv	TAAAGCTCGTCCATACCGCC	
267	mNeonGreen fw	TCTACGAAGGGGGATCTGCA	276 bp
268	mNeonGreen rv	TGAGTTCGTCATCACTGGGC	
269	mNeonGreen fw	CCAAATGACGGCTACGAGGA	209 bp
270	mNeonGreen rv	GTCAGTGAAGCCCCATCCTC	

Movie S1

Example of cell shrinkage after FRET loss in cultured B cells. Splenic B cells were purified from Igκ^{INDIA} transgenic mice, activated in vitro with LPS and IL-4, and imaged every 60 s for FRET loss at 37°C after addition of staurosporine. Images feature a single INDIA^{+} B-cell over time (yellow, FRET^{+}; green, FRET$^{–}$; scale bar: 10 μm). Cell shrinkage and necrosis are observed after FRET loss.

Movie S2

Example of motility arrest and blebbing after FRET loss in cultured B cells. Splenic B cells were purified from Igκ^{INDIA} transgenic mice, activated in vitro with LPS and IL-4, and imaged every 60 s for FRET loss at 37°C after addition of staurosporine. Images feature a single INDIA^{+} B-cell over time (yellow, FRET^{+}; green, FRET$^{–}$; scale bar: 10 μm). Irregular cell shaping, shrinkage, arrested motility, blebbing and necrosis are observed after FRET loss.

Movie S3

Example of blebbing after FRET loss in cultured B cells. Splenic B cells were purified from Igκ^{INDIA} transgenic mice, activated in vitro with LPS and IL-4, and imaged every 60 s for FRET loss at 37°C after addition of staurosporine. Image centers feature an INDIA^{+} B-cell over time (yellow, FRET^{+}; green, FRET$^{–}$; scale bar: 10 μm). Blebbing, irregular cell shaping and necrosis are observed after FRET loss.